

Have Superheavy Elements been Produced in Nature?

I. Petermann¹, K. Langanke^{2,3,4}, G. Martínez-Pinedo^{3,2}, I. V. Panov^{5,6}, P.-G. Reinhard⁷, and F.-K. Thielemann⁵

¹ Argelander-Institut für Astronomie, Universität Bonn, Auf dem Hügel 71, D-53121 Bonn, Germany

² GSI Helmholtzzentrum für Schwerionenforschung, Planckstraße 1, D-64291 Darmstadt, Germany

³ Technische Universität Darmstadt, Institut für Kernphysik, Schlossgartenstr. 2, D-64289 Darmstadt, Germany

⁴ Frankfurt Institute for Advanced Studies, Frankfurt, Ruth-Moufang Str. 1, D-60438 Frankfurt, Germany

⁵ Department of Physics, University of Basel, Klingelbergstr. 82, 4056 Basel, Switzerland

⁶ Institute for Theoretical and Experimental Physics, B. Chermushkinskaya St. 25, 117259 Moscow, Russia

⁷ Institut für Theoretische Physik II, Universität Erlangen-Nürnberg, Staudtstrasse 7, D-91058 Erlangen, Germany

November 9, 2018

Abstract. We discuss the possibility whether superheavy elements can be produced in Nature by the astrophysical rapid neutron capture process. To this end we have performed fully dynamical network r-process calculations assuming an environment with neutron-to-seed ratio large enough to produce superheavy nuclei. Our calculations include two sets of nuclear masses and fission barriers and include all possible fission channels and the associated fission yield distributions. Our calculations produce superheavy nuclei with $A \approx 300$ that however decay on timescales of days.

PACS. 26.30.Hj r-process – 27.90.+b Properties nuclei with $A \geq 220$ – 25.85.-w Fission reactions

1 Introduction

More than 40 years ago, the possible existence of an island of superheavy nuclei was proposed (see e.g. Refs. [1, 2, 3]), due to the appearance of shell closures of protons and neutrons at mass numbers beyond the then available nuclear data. Various models predicted shell closures at $Z = 114$ and $N = 184$ [3, 4, 5, 6, 7]. More recent microscopic calculations [8, 9, 10, 11, 12] suggest that the magic proton number could be higher than $Z = 114$ (possibly $Z=120$, 124 or 126) and the neutron shell closure occurs at $N = 172$ or 184. In fact, shell closures are somewhat washed out to regions of shell stabilization around these numbers [13]. Shell closures make superheavy nuclei stable against the dominating decay channel in this region: spontaneous fission. The highest fission barriers are expected for nuclei just above the closed proton shell ($Z = 114$) and just below the closed neutron shell at $N = 184$. This is of high relevance for the decay half-life of beta-stable nuclei in this mass region [14, 15, 16, 17, 18].

Over the last thirty years, several experimental campaigns at Berkeley, GSI, RIKEN, and JINR Dubna have explored this predicted island of superheavy elements of increasingly stable nuclei around atomic number 114 (see e.g. [19, 20, 21, 22, 23]) and have found by now elements with charge numbers up to $Z = 118$ [24, 25, 26]. The decay chains observed so far suggest the existence of a region of enhanced stability created by shell effects. Alpha-decay

chains with fission, occurring at the end of the chain, explored the boundary of the island at low Z and N . The question remains now how far the island extends in the other directions (low Z , high N ; high Z , low N ; high Z , high N) and what experimental paths can lead us to these regions.

A related question has been addressed almost as long, i.e. whether superheavy elements are/could be produced in Nature [27, 28]. The only candidate process for astrophysical nucleosynthesis of these heavy elements is the r (apid neutron capture) process (for reviews see [29, 30, 31]). Alternative terrestrial, non-accelerator, experiments have been discussed [32, 33, 34, 35, 36].

While the very early discussion made it plausible that superheavy elements can be produced in r-process nucleosynthesis [27], more systematic approaches, including neutron-induced fission estimates, predicted that the r-process path would reach areas dominated by fission and the path to superheavy elements would be blocked in nature, dependent, however, on mass model uncertainties [37, 38, 39, 40].

The first extended table of fission barrier predictions by Howard and Möller [41] permitted to engage in more systematic calculations. Thielemann, Metzinger and Klapdor [42] performed beta-delayed fission calculations for a number of mass models in combination with the above fission barrier predictions. In their application to r-process calculations [43], they came to the conclusion that the r-process path ends in a 100% beta-delayed fission region and superheavies cannot be reached. Their results

Send offprint requests to:

were based on a combination of the Hilf mass formula [44] (which contains a slightly too steep mass parabola) and the Howard and Möller [41] fission barriers, which by now turn out to be somewhat underestimated [45]. The combination of both effects led to an overestimation of the effect of fission [29] in the r-process path around $Z = 92$.

Since then, after considering these deficiencies, studies aimed at using r-process nuclei for cosmochronometry have neglected fission [46] and did not address the question of production of superheavy nuclei. In recent years improved predictions of fission barrier tabulations for extended ranges of nuclei have become available [47, 48, 15, 49], being based on the Extended Thomas-Fermi (ETFSI), Thomas-Fermi (TF), Finite Range Droplet Model (FRDM) or the Hartree-Fock Bogoliubov (HFB) approach. This also led to new neutron-induced fission and beta-delayed fission calculations [50, 51] that permitted to address the formation of superheavy elements and long-lived cosmochronometers. In order to explore these issues we have performed a new set of r-process calculations with few preliminary results reported in [52, 53, 54]. In this manuscript, we present detailed calculations aiming to answer the following questions: (i) is the r-process experiencing strong fission effects during the build up of heavy nuclei by neutron captures and beta-decays or can unstable extremely neutron-rich nuclei with mass numbers up to $A = 300$ and beyond be produced? (ii) Does the subsequent decay to beta-stability pass by areas of the nuclear chart where fission dominates, hence blocking the production of long-lived superheavy nuclei? (iii) Can this area of fission dominance be surpassed during the r-process towards higher charge numbers, so that subsequent beta-decay ends with finite abundances in the valley of beta-stability, followed by alpha-decay chains towards the island of superheavy nuclei? This three options/questions are indicated in Fig. 1.

Our paper is structured in the following way. Section 2 discusses the nuclear input used: masses and fission barriers of nuclei far from stability. Section 3 discusses the r-process model and presents the results of the nucleosynthesis calculations. Section 4 analyzes the results addressing the reliability of the nuclear input due to comparison with data. Section 5 presents the conclusions.

2 The Role of Masses and Fission Barriers

If one wants to address the question whether the island of superheavy elements was reached in natural neutron capture environments, like final products of r-process nucleosynthesis, a complete knowledge of all possible reaction and decay properties is required. This includes neutron capture, photo-disintegration, neutron-induced fission, beta-decay, beta-delayed fission, spontaneous fission and for sufficiently large temperatures gamma-induced fission. In order to provide this information in unknown territory, theoretical prediction are required. Prediction of these properties rely therefore on masses (to determine reaction Q-values), fission barriers, optical potentials for transmission coefficients of particle channels, transmission coefficients for gamma-transitions (determined ei-

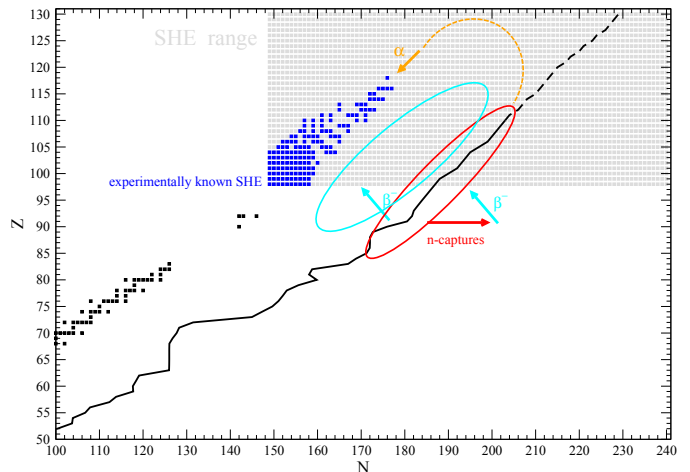


Fig. 1. Possible pathways of the r-process in the nuclear chart (solid line). On the path and the subsequent decay back to beta-stability there exist three options to encounter or avoid fission on the way to superheavy nuclei (options i)-iii) in the text). In option iii) superheavies would be made by producing progenitors with even higher charge numbers which then decay by subsequent beta- and alpha-decays. The present investigation, limited to network calculation up to $Z=110$, cannot explore this latter option.

ther from giant resonance properties or microscopic approaches), level densities of excited states (obtained from back-shifted Fermi gas or combinatorial approaches) [49, 51, 55, 56, 57, 58, 59, 60, 61, 62, 63]. Spontaneous fission has been described with different levels of sophistication including: a simple formula fitted to experimental data [64, 65], macroscopic-microscopic approaches [15, 66, 67], and Skyrme-Hartree-Fock approaches [18, 49].

For a number of years extended and increasingly reliable mass predictions have been available, the Finite Range Droplet Model (FRDM) [68], the Extended Thomas Fermi Model with Strutinski Integral (ETFSI) [69], the “microscopic” Dufo-Zuker mass formula [70], and the Hartree-Fock-Bogoliubov approach with Skyrme functionals [71, 72]. Relativistic and non-relativistic mean field approaches which do not yet reach an accuracy level in ground state masses of 0.6–0.7 MeV have not been considered in r-process simulations.

Global predictions of fission barriers have been scarce. After the Howard and Moller [41] predictions (which are now known to produce too small barriers), new attempts have only been performed in the last decade [15, 18, 47, 48, 49, 63, 73].

They are based on the ETFSI model [47], the Thomas-Fermi approach [48], with a similar macroscopic mass parabola as FRDM, combined with shell corrections of the Finite Range Liquid Drop model FRLDM [15] - similar, but not identical to FRDM, and the Skyrme-Hartree-Fock-Bogoliubov model [49, 63] based on the density functional used for the HFB-14 masses [74]. The Skyrme Hartree-Fock approach has also been used for a sensitivity study of fission barriers for superheavy nuclei [18] and for the dependence of the fission barrier on excitation energy [73].

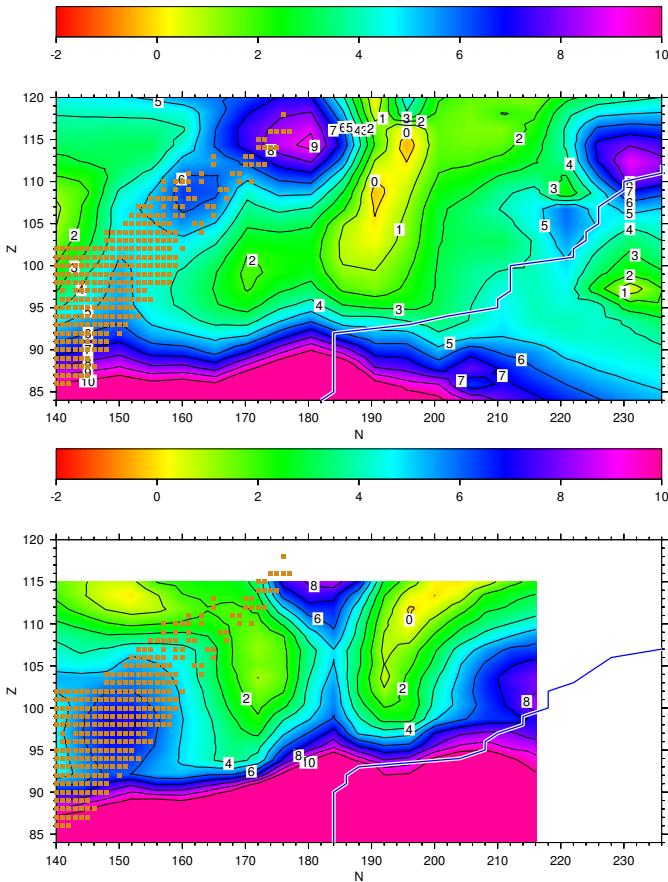


Fig. 2. Contour plots of the largest fission barrier heights from the TF (top) [48] and ETFSI (bottom) [47] mass models. This figure also indicates to which extent data sets are available in the nuclear chart. HFB barriers are only publicly available in the range $Z = 90$ – 102 [49] and FRDM barriers [15] only close to stability.

Fig. 2 shows contour plots of the largest fission barrier for individual nuclei from the TF (top) and ETFSI (bottom) models. The calculation of beta-delayed or neutron-induced fission requires the knowledge of mass differences that should be derived consistently from the same model as the barriers [46]. Unfortunately this is not always possible, however based on the similarity of the underlying model we expect that the most reasonable combinations for barriers and masses are ETFSI/ETFSI, TF/FRDM, FRLDM/FRDM, and HFB-14/HFB-14. Of these four sets only two (ETFSI/ETFSI, TF/FRDM) can currently be used for global r-process calculations which require knowledge of nuclear properties from stability to the neutron drip line for an extended range of Z values. The Bruslib database of astrophysical reaction rates¹ includes fission barriers based on the HFB-14 model for the range $Z = 90$ – 110 and neutron induced rates up to $Z = 102$. The recent FRLDM barriers [15] cover the range $Z = 78$ – 125 but always close to the beta-stability line.

¹ <http://www.astro.ulb.ac.be/bruslib>

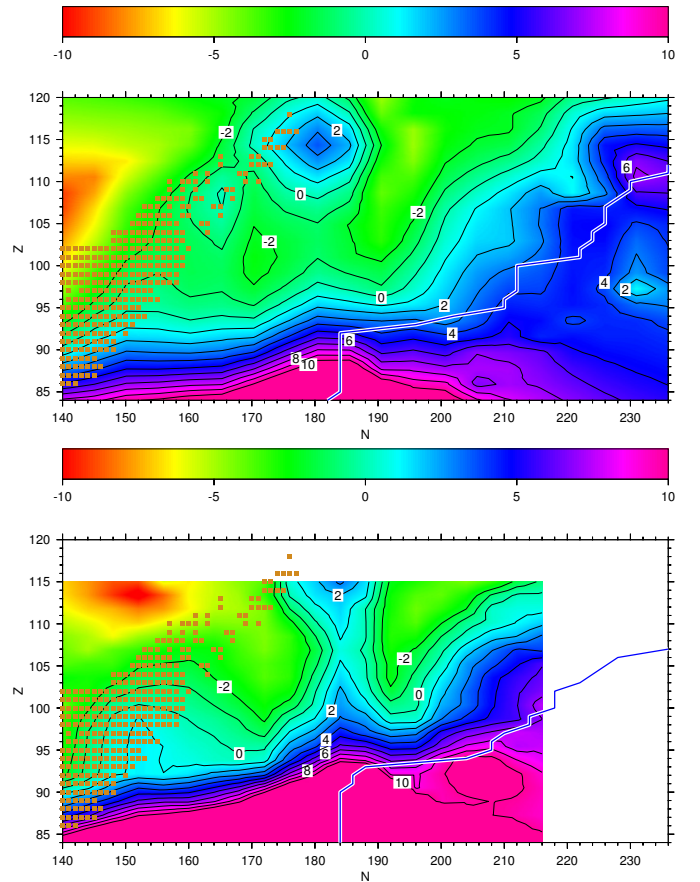


Fig. 3. Contour plots of $B_f - S_n$ for the combinations TF/FRDM (top) and ETFSI/ETFSI (bottom). While there exist positive values of $B_f - S_n$ for neutron numbers around $N = 184$ also for $Z > 95$ in the bottom figure (indicating that neutron-induced fission is not permitted), this is not the case for TF/FRDM. The neutron-drip line is shown for the appropriate mass modes (FRDM and ETFSI). It can be seen that in the vicinity of the neutron-drip line neutron-induced fission is clearly inhibited.

In figures 3 and 4 we present the different reaction and decay properties for neutron-induced, beta-delayed and spontaneous fission. Figure 3 shows contour plots of the difference between fission barrier and neutron separation energy, $B_f - S_n$. Nuclei for which this value is below 2 MeV are expected to fission immediately after capturing a neutron. Given the fact that fission barriers do not suffer from strong odd-even effects while the neutron separation energies are affected by those, we expect that neutron-induced fission will mainly occur for even- N r-process nuclei.

Figure 4 shows the dominant decay channel (alpha-decay on the neutron-deficient side of stability, beta-decay, beta-delayed fission in regions where the beta-decay Q -value is larger than the fission barrier of the daughter nucleus, and spontaneous fission), see also [50, 51, 54, 75]. As the TF barriers provide only information about the height of the largest barrier we have estimated the spontaneous fission half-lives using the simple parametrization of Ref. [64], but with coefficients adjusted to the avail-

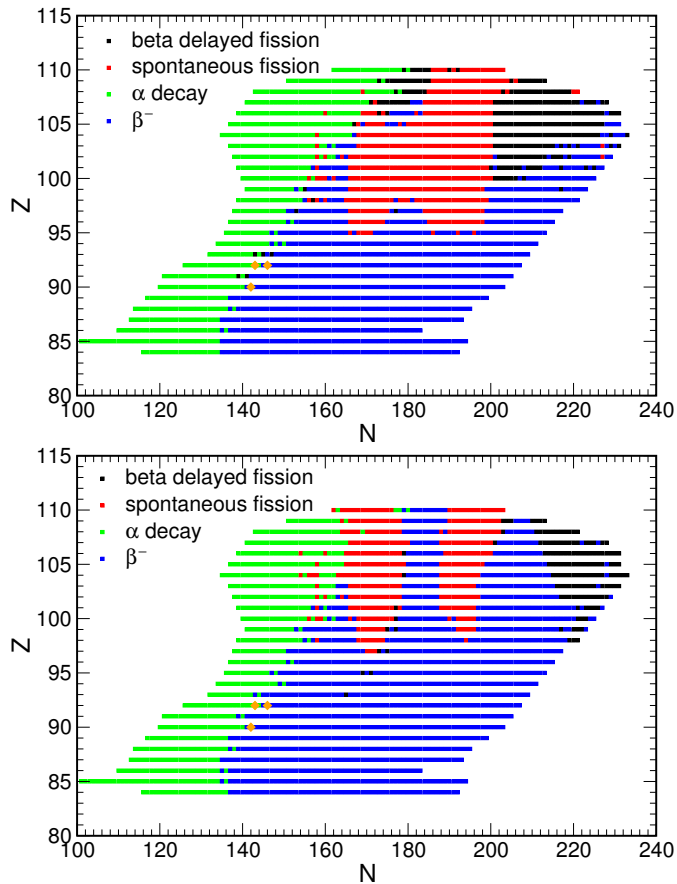


Fig. 4. Dominant decay channels: alpha-decay on the proton-rich side of stability - not of importance here, beta-decay, beta-delayed fission in regions with positive $Q_{\beta} - B_f$ (*daughter*) and regions where spontaneous fission half-lives are shorter than beta-decay half-lives.

able experimental fission half-lives related to the TF fission barriers:

$$\log t_{1/2}(\text{s}) = 8.08B_f - 24.05, \quad (1)$$

where the barrier B_f is given in MeV. We use the same parameters for the ETFSI barriers so that for the same barrier both models predict the same spontaneous fission half-life. Alpha-decay half-lives are obtained using the Viola-Seaborg semi-empirical relationship between half-life and alpha decay energy with parameters determined in ref. [76]. We use beta-decay half-lives and beta-delayed neutron emission probabilities from ref. [77] which are currently the only values available for the mass range of interest here. As these data only extend to $Z = 110$, this is the upper limit for our r-process network. Whenever an experimental half-life is known we use this value in our calculations.

Beta-delayed fission rates are determined based on the FRDM beta-decay rates [77] using an approximate strength distribution for each decay based on the neutron-emission probabilities. For each fissioning nucleus and fission channel the fission yields, including the amount of neutrons

produced, are determined [78] using the statistical code ABLA [79,80].

While there are obvious differences for fission barrier predictions of the different models shown in Fig. 2, they become more prominent in $B_f - S_n$ (Fig. 3) and the prominent decay channels as shown in Fig. 4, especially close to the neutron shell closure $N = 184$. The content of Figs. 3 and 4 provides the information for judging which decay/reaction channel is dominant in a particular region. However, the determination of the neutron-induced fission rate requires also the knowledge of the neutron density, n_n , of an r-process environment. One important result is that $B_f - S_n$ is always positive close to the neutron-drip line, independently of the mass model. This is expected as the fission barriers increase while the neutron separation energies decrease towards the neutron drip line. This means that an r-process does not experience strong neutron-induced fission if proceeding close to the drip line for $N < 184$. However, at the $N = 184$ magic shell the drip line moves closer to beta-stability and the quantity $B_f - S_n$ becomes smaller. For the TF/FRDM model, its value is around 2 MeV for nuclei around $Z \sim 94$, $N \sim 186$ for which the neutron-induced fission dominates over the (n, γ) channel. This inhibits the production of heavier nuclei, due to neutron-induced fission. The ETFSI/ETFSI model predicts values of $B_f - S_n \approx 8$ MeV in the same region, remaining large along the r-process path to heavier nuclei. The build up of heavy nuclei continues and only ends by beta-delayed fission in the region $Z \sim 105$, $N \sim 220$, see black region in figure 4. Notice that both models predict very similar neutron separation energies but rather different fission barriers.

In the range of elements up to $Z = 115$, regions dominated by spontaneous fission will always be encountered during the decay to beta-stability. For the TF/FRDM case this is unavoidable, as an extended and connected region dominated by spontaneous fission has to be passed. In the ETFSI/ETFSI case, the spontaneous fission region is split into two “islands” divided by a range of about 10 units in neutron number around $N = 184$, where beta-decay dominates without being followed by delayed fission. Thus, beta-decay back to stability will have the chance to proceed through the channel between the islands, until it encounters the region with $N < 184$. Dependent on the beta-decay half-lives encountered, superheavy nuclei could exist for an extended period of time before fissioning. We cannot make statements for a possible production of nuclei beyond $Z = 110$ as this is the upper limit of our present network calculations due to the restricted availability of the nuclear input. For this region extended sets for theoretical predictions have been published [18] after finishing our calculations and in the future we plan to explore their impact in r-process nucleosynthesis.

The decay and reaction inputs discussed in this section and displayed in Figs. 2, 3 and 4 provide the basis for applications to the r-process calculations given in the following section.

3 r-Process Calculations with fission

3.1 Astrophysical Sites

A high availability of neutrons, leading to a large ratio of neutrons to seed nuclei (typically Fe-group nuclei or beyond, up to $A = 80$) can occur in two types of explosive astrophysical environments: (a) Very neutron-rich material, which is obtained under high nuclear matter/neutron star densities, where electron capture on protons by degenerate electrons with high Fermi energies cause a proton-to-nucleon ratio Y_e of about 0.1, is ejected and leads to an r-process during the expansion phase. Possible examples are the ejecta from neutron star collision events, [81,82,83,84], or other environments ejecting highly neutronized material like fast rotating core collapse supernovae with strong magnetic fields and jet ejecta [85,86,87]. (b) Matter which is only slightly neutron-rich but experiencing a fast expansion and high entropies. In such a case the reactions ${}^4\text{He}(\alpha\alpha, n){}^9\text{Be}(\alpha, n){}^{12}\text{C}$ and/or ${}^4\text{He}(\alpha\alpha, \gamma){}^{12}\text{C}$ are responsible to move matter from ${}^4\text{He}$ to ${}^{12}\text{C}$ followed by a fast sequence of reactions producing heavier seed nuclei and few neutrons remaining. At high entropies, $\propto T^3/\rho$, three body reactions are suppressed due to the low density and/or high number of photons hindering the production of heavy seed nuclei and result in large amounts of ${}^4\text{He}$ (with $N = Z$) and a tiny amount of heavy seed nuclei. This results in large remaining neutron-to-seed ratios. Examples of this case are the neutrino-driven wind [88,89,90,91,92,93,94,95] from the nascent proto-neutron star after supernova core collapse (provided that it can produce neutron-rich ejecta [96,97]) and matter ejected from accretion disks around black holes [98,99].

In the above two options, the high neutron-to-seed ratio is the dominant driving force behind a rapid neutron capture (r-)process. However, dependent on the environment, the densities and temperatures can vary and cause differences in the exact working of the r-process. In order to produce nuclei as heavy as Uranium and Thorium which are only produced by the r-process, one requires conditions with neutron-to-seed ratios of the order of 150.

3.2 r-Process model calculations

The previous subsection outlined the still existing uncertainties in astrophysical sites/conditions which will then also be affected further by nuclear uncertainties discussed in section 2. We stress that, independent of the actual environment, the decisive feature of an r-process to produce superheavy elements is a sufficiently high neutron-to-seed ratio. In the following, we assume assumed conditions corresponding to fast expanding ejecta with high entropy, in order to ensure a large enough neutron-to-seed ratio.

We start our calculations at a temperature of 10 GK for which Nuclear Statistical Equilibrium is applicable and assume that the matter follows a homologous adiabatic expansion where the density behaves as:

$$\rho(t) = \rho_0 \exp(-t/\tau). \quad (2)$$

We use $\tau = 3$ ms following the hydrodynamical simulations of ref. [100]. At later times hydrodynamical simulations show that the evolution is not anymore homologous and can be approximated by [101,102,103]:

$$\rho(t) = \rho_1 \left(\frac{\Delta + t_1}{\Delta + t} \right)^2, \quad (3)$$

where the parameter Δ represents the time scale on which the matter evolves from conditions of almost constant density ($t \ll \Delta$) to constant velocity ($t \gg \Delta$) [95]. We use a value of $\Delta = 2$ s in agreement with hydrodynamical simulations [100,96].

In order to attain a large neutron-to-seed ratio we assume a constant entropy of 200 k /nucleon and initial $Y_e = 0.35$ that results in a neutron-to-seed ratio of 290 at 3 GK. The temperature is determined by the condition of constant entropy using the equation of state of ref. [104]. Our network code is based on the XNet code of ref. [105] that has been extended to treat implicitly all fission reactions.

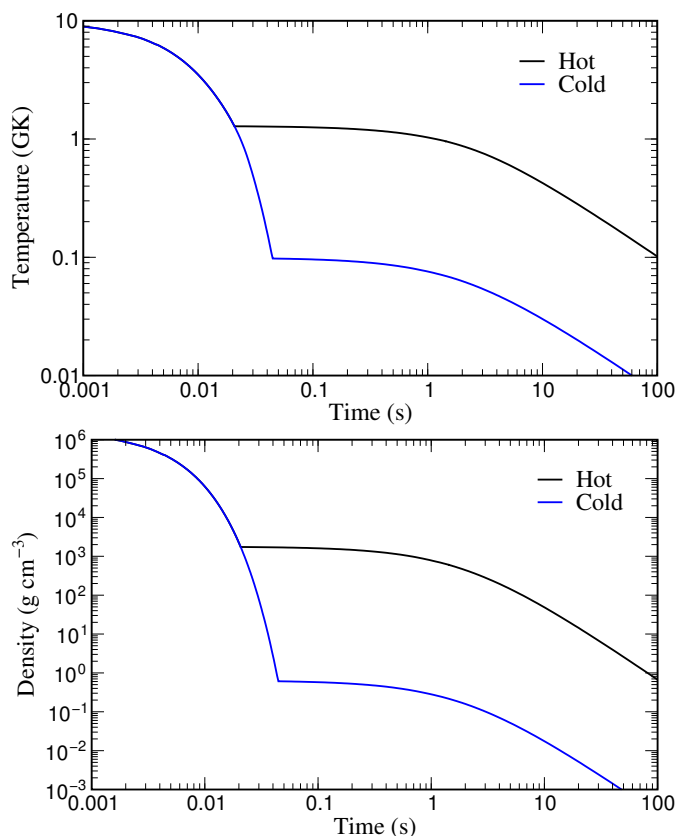


Fig. 5. Evolution of temperature and density for a hot and cold r-process depending on the choice of t_1 in Eq.(3). Notice that for both cases the n /seed ratio drops below 1 in the range $t=1-2$ s.

As discussed in section 3.1, the r-process can occur under quite different astrophysical conditions. In the following, we present two extreme cases for the late time evolution (see figure 5) by choosing t_1 as the time for which

the temperature has reached values of 1.15 and 0.1 GK, respectively. In the following, we refer to these two cases as “hot” and “cold” r-process.

The nucleosynthesis in these two cases differs in two major aspects. First, in the “hot” r-process calculations, we find that there is a continuous production of seed nuclei during the whole duration of the r-process as charged-particle reactions never completely freeze-out (see ref [106]). This is not the case in the “cold” r-process, as for such low temperatures charged-particle reactions are too slow when compared with the dynamical timescale of r-process nucleosynthesis. The continuous production of seed nuclei manifests itself in enhanced abundances for nuclei in the range $A = 20\text{--}90$. This is demonstrated in figure 6 that shows the final r-process abundances based on the TF/FRDM input. Calculations with the ETFSI/ETFSI input show the same features.

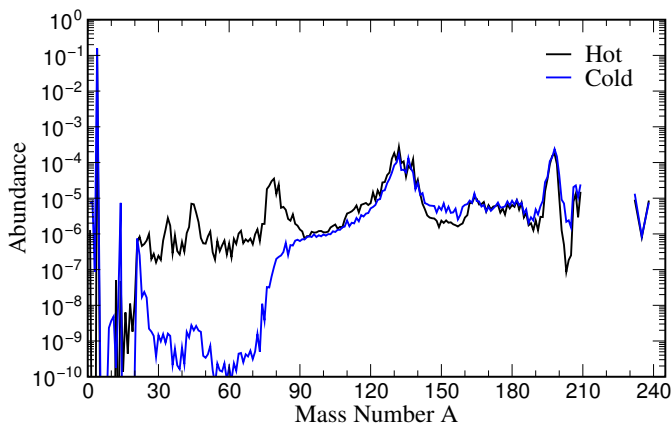


Fig. 6. Final abundances for the hot and cold r-process scenarios after 1 Gy; i.e. after the decay of unstable isotopes (see text for details).

The second difference relates to the role of photodisintegration reactions during the r-process. At the larger temperatures of the hot r-process the photodisintegration reactions are fast enough to establish a $(n, \gamma) \rightleftharpoons (\gamma, n)$ equilibrium. This chemical equilibrium between both reaction types along an isotopic chain, defines a narrow “r-process path”, with a nucleus of dominant abundance in each chain, acting as waiting point for beta-decays. This is the “classical” r-process picture as introduced in ref. [107, 108].

In the “cold” r-process, photodisintegration is too slow to establish an equilibrium with neutron captures. The evolution is rather determined by neutron captures and competing beta-decays which opposite to photo-dissociation do not vary much from isotope to isotope under r-process conditions. As a consequence several nuclei in each isotopic chain are substantially populated which leads to a broader r-process path. Calculations in the cold r-process scenario have been already presented in [109, 110, 95], however, with different aims than discussed here.

Besides this more general discussion, addressing the working of the r-process, we want to concentrate now on

the focus of the present investigation, the effect of fission and the path to superheavy nuclei. For this purpose we have performed calculations in the hot and cold r-process scenarios using the TF/FRDM and ETFSI/ETFSI input sets. We focus in the following on the mass regime $A > 180$ that is relevant for our discussion. The abundance distribution at the moment where the neutron-to-seed ratio reaches 1, marking the beginning of neutron-capture freeze-out, is shown in figs. 7 and 8. In each case a comparison is given between a hot and a cold r-process, shown in Fig. 7 for a nuclear input set TF/FRDM for fission barriers and masses and in Fig. 8 for the set ETFSI/ETFSI.

We see that in both cases (hot and cold r-process) and for both sets of nuclear input the abundances decline substantially for nuclei $A > 280$, extending in the cold case for a few more mass units. As discussed by [38, 109] in a hot r-process $(n, \gamma) \rightleftharpoons (\gamma, n)$ equilibrium ensures a substantial leakage into the fission channel, hindering the production of heavier elements once an isotopic chain is reached where neutron-induced fission can occur. This occurs in the region $Z = 95\text{--}100$ close to or slightly beyond $N = 184$, where as seen in Fig. 3 $B_f - S_n < 2$ MeV. Once neutrons are exhausted, Fig. 4 (top) shows that spontaneous fission can become the dominating fission channel. In the cold r-process scenario the evolution is dominated by individual nuclei with low fission rates, allowing the production of heavier nuclei than in the hot scenario.

To explore the dependence on the nuclear input, figs. 9 and 10 show the evolution of fission rates for the different channels for a hot and cold r-process using the fission rates and masses TF/FRDM and ETFSI/ETFSI. There are several general features that are worth to be mentioned. During the r-process phase, defined by a neutron-to-seed ratio larger than one, neutron-induced fission dominates. Once the neutron-to-seed becomes smaller than one and the r-process freeze-out starts, the rate of neutron-induced fission suddenly decreases. At this moment, the r-process material starts to beta-decay to stability, producing beta-delayed neutrons via beta-delayed neutron emission that can induce neutron-captures but also neutron-induced fission. The latter is particularly important for the matter accumulated at $N = 184$ ($A \sim 280$) that during the beta-decay to the stability feeds the region with $Z \sim 95$, $N \sim 175$ where neutron-induced fission can operate again, see fig. 3. This revival of neutron-induced fission is seen in all the calculations by a second hump that is delayed by the time scale of the successive beta decays. Once neutron-induced is revived it sustains itself by a mechanism similar to a chain reaction and continues to be the dominating channel till the neutron density becomes too low at times around several tens of seconds when beta-delayed fission and spontaneous fission dominate. Spontaneous fission, which is dominant for nuclei closer to stability, is always less important during the working of the r-process, but becomes larger in the freeze-out phase, when the path moves closer to stability. In the cold case the path is more spread out in abundances, as discussed above, and encounters, therefore, the spontaneous fission region (closer to stability) earlier, already before the decay back to sta-

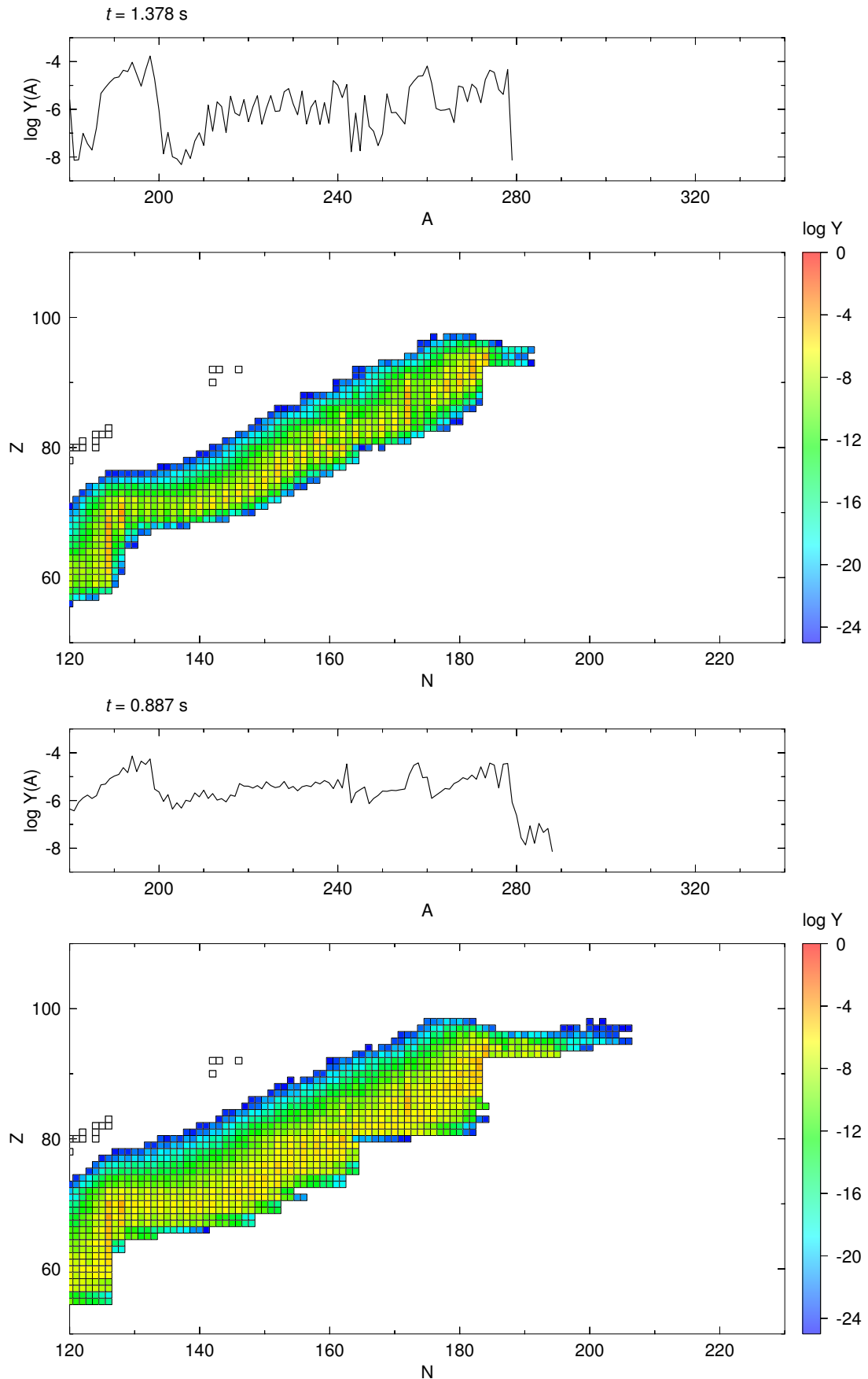


Fig. 7. Results from calculations for hot (top) and cold (bottom) r-process conditions, utilizing fission barriers and mass predictions from the models ETF and FRDM. In both cases the abundances are shown as a function of A as well as in terms of a contour plot, where the abundances of nuclei are indicated by their color. The abundances are given at the point of neutron freeze-out, i.e. when the ratio of neutrons to heavy nuclei has dropped down to 1. That means that on average each nucleus will not capture more than one neutron after this point in time.

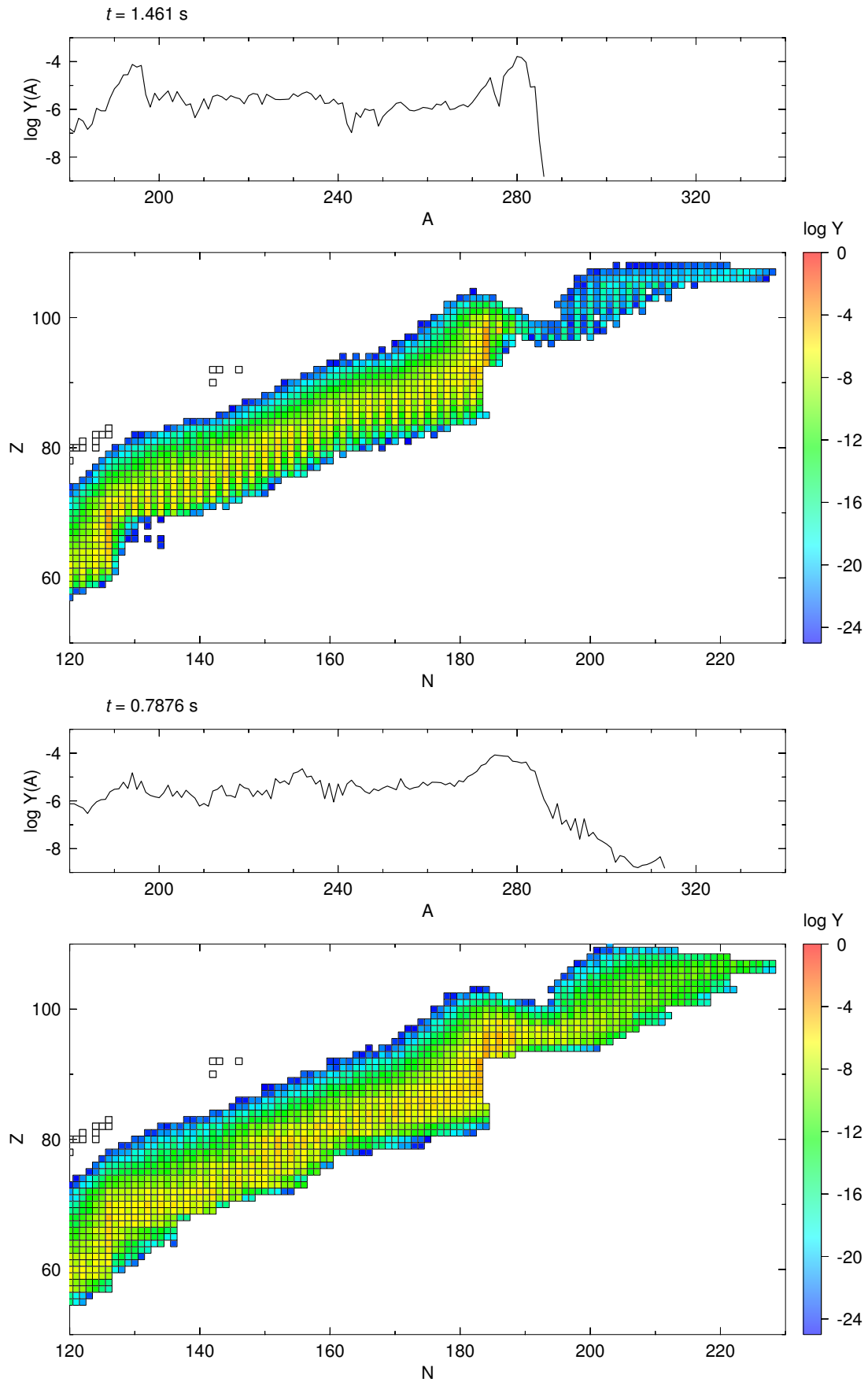


Fig. 8. Same as Fig. 7, but utilizing the ETFS/ETFSI combination of fission barrier and mass predictions. It can be seen that the evolution proceeds to higher masses than in Fig. 7 and fission is less important during the working of the r-process. See text for a discussion.

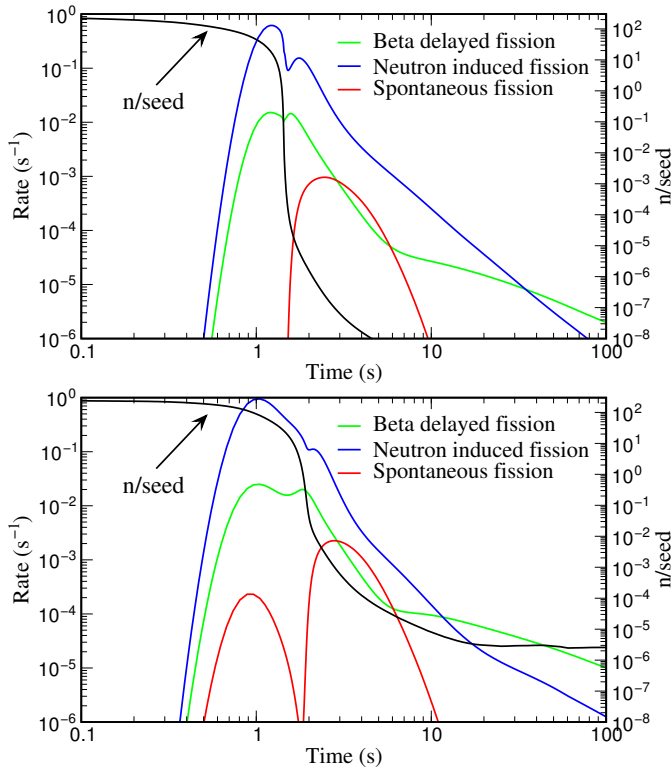


Fig. 9. The evolution of fission rates for the different channels shown for a hot (top) and cold (bottom) r-process with the fission barrier/mass model selection TF/FRDM.

bility sets in. For nuclei with the highest mass numbers (see also Fig.(4)) beta-delayed fission can also be important at late times.

While for TF/FRDM nuclear input we have seen that neutron-induced fission prevents the build-up of (super)heavy elements, the situation looks different when applying ETFSI for fission barriers and masses (see Fig. 8). This is understandable from Fig. 3, where we see that the region with $B_f - S_n < 0$ is further removed from the drip-line (and r-process path) than for the TF/FRDM case. As beta-delayed fission is always less prominent than neutron-induced fission during the r-process build-up, we also expect matter to continue to proceed to elements heavier than those included in the present calculation (see sect. 2). The relative role of the three fission channels shown in Fig. 10 is similar to that shown in Fig. 9, but with the exception that neutron-induced and beta-delayed fission do not fully hinder the production of nuclei heavier than those included in the present network, limited to $Z \leq 110$. Another difference is that spontaneous fission becomes more prominent in the late freeze-out phase when the path moves closer to stability. This can be understood as neutron-induced and beta-delayed fission do not fully prevent the production of heavy nuclei.

It was already realized from Fig. 4 that the area where spontaneous fission dominates is split for the ETFSI/ETFSI case, leaving a “free passage” in the vicinity of $N = 184$ [52]. This permits beta-decay in the direction of the valley of stability. The decay path will encounter, however, the

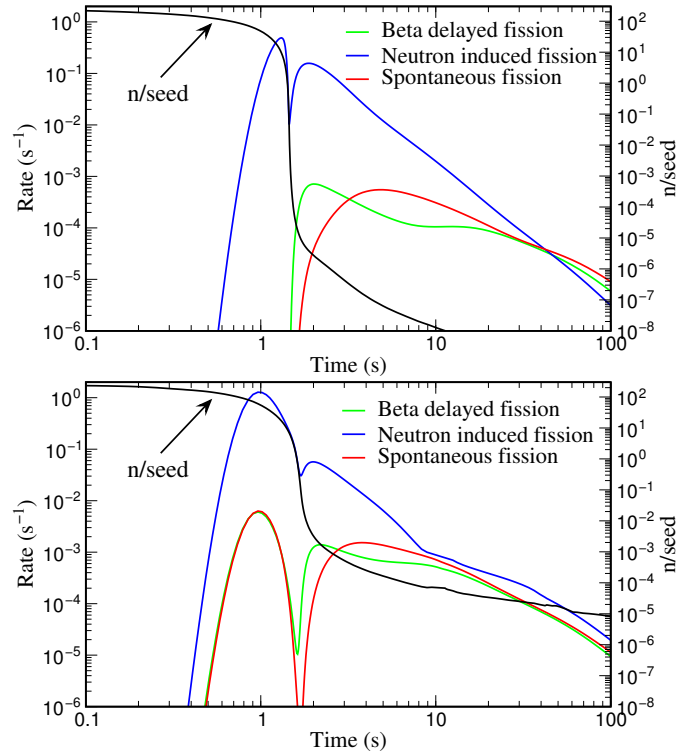


Fig. 10. Similar to Fig. 9, the evolution of fission rates for the different channels shown for a hot (top) and cold (bottom) r-process, but with the fission barrier/mass model selection ETFSI/ETFSI.

lower of the two spontaneous fission islands, at a charge number $Z > 110$, i.e. outside the limits of the presently used nuclear network.

Fig. 11 shows (for the ETFSI/ETFSI combination of fission barriers and masses) results of hot and cold r-process calculations at that point in time when $Z=109$ nuclei are still present or just decayed to $Z=110$, i.e. when reaching the limits of the nuclear network in the late decay phase. In both calculations this happens after about 12h. Thus, when utilizing ETFSI/ETFSI fission barriers and masses, such (superheavy) nuclei exist for this amount of time. From Fig. 4 we know, however, that they will finally also reach the lower island of spontaneous fission and not reach the valley of stability as final destination.

As noticed above in the ETFSI/ETFSI case the r-process involves nuclei heavier than those included in our network and consequently we cannot determine the answer to question (iii) of the introduction, i.e. the possibility of producing nuclei heavy enough to circumvent the region of fission dominance also during the decay to stability. This option is not available for the TF/FRDM case as sufficiently heavy nuclei are never produced during the r-process.

4 Discussion and Summary

In this paper we examined whether superheavy elements can be synthesized in nature by the r-process. As the r-

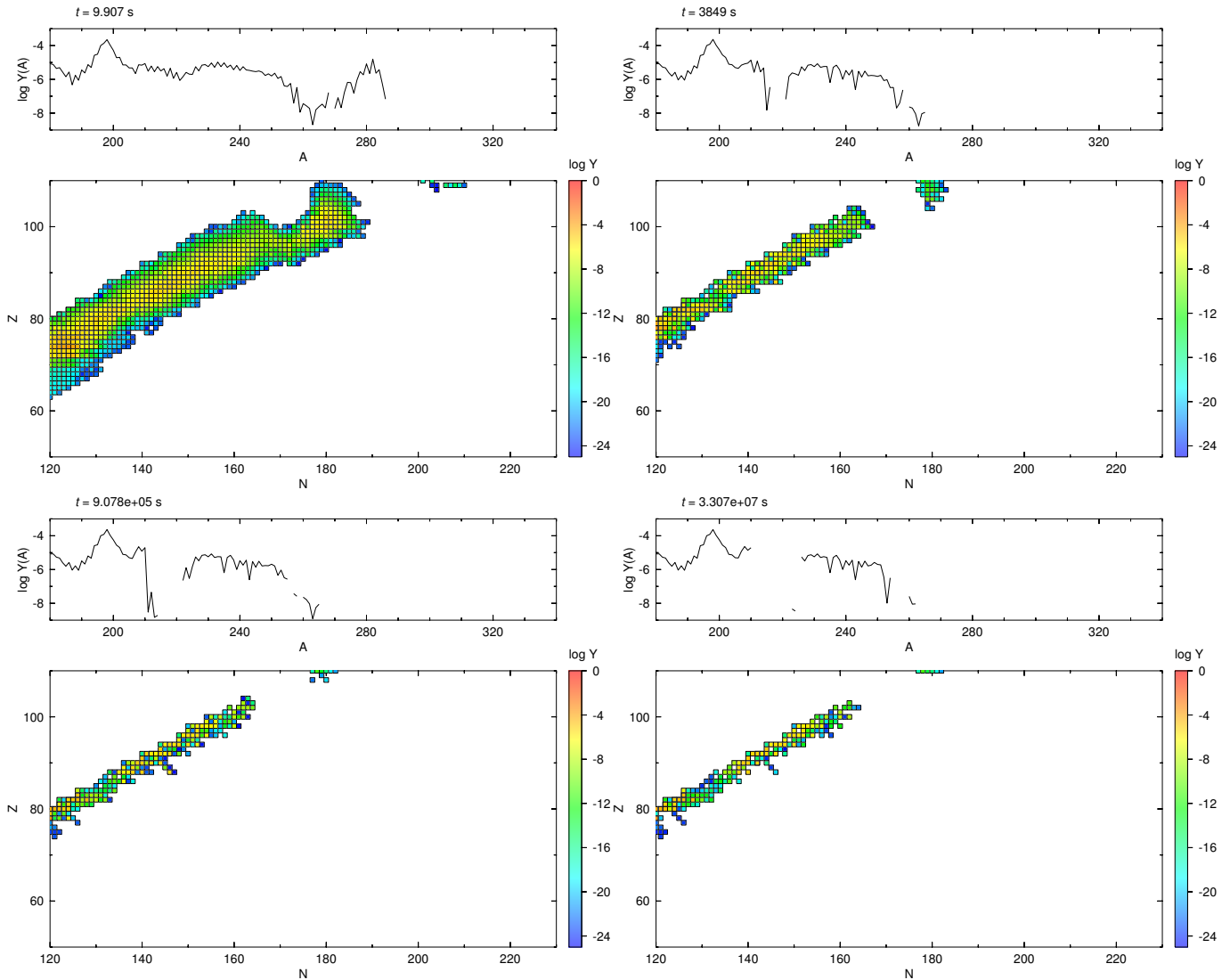


Fig. 11. Top and bottom figures show the abundance patterns of hot and cold r-process calculations with ETFST/ETFSI fission barriers and masses. The plots refer to the latest point in time when still $Z=109$ nuclei are present, or just have decayed to $Z=100$. These are the results of decay via the "free passage" region of spontaneous fission shown in Fig. 4.

process conditions in astrophysical explosions are not fully understood, we utilized two sets of calculations, relating to the so-called hot and cold environments, where either photo-disintegrations play or do not play an important role. For conditions with sufficient neutron-to-seed ratios to produce actinide and heavier nuclei, we came to essentially two types of conclusions.

For one set of fission barriers and mass predictions (TF/FRDM) the r-process is terminated by neutron-induced and beta-delayed fission before superheavy nuclei can be reached. For the other set (ETFSI/ETFSI) neutron-induced and beta-delayed fission do not prevent the build-up of superheavy nuclei even extending beyond $Z > 110$. Unfortunately, this is the edge of our network calculations, related to the current limits of available global nuclear input. Independent of this shortcoming, our calculations predict that nuclei with masses of the order $A = 290$ are produced and survive for about 12 hours after an r-process event

(which only takes seconds). After several beta decays also these nuclei will encounter regions of spontaneous fission an decay to medium mass nuclei before reaching the valley of stability.

The present investigation is another example showing the importance of nuclear input for r-process nucleosynthesis. A reduction of the underlying uncertainties by either experiment or theory is desirable. This should also include an extension of the calculations to nuclei with higher charge, $Z > 110$, and neutron number to determine if the r-process can produce progenitors with such high mass numbers that during the decay to the stability it can circumvent the region of fission dominance predicted by current models ($N \sim 184, Z > 100$). A first step towards this goal has been achieved in a recent study [18], which shows that within the uncertainties among different Skyrme functionals it is likely that spontaneous-fission will hinder the production of elements beyond $Z = 120$.

We acknowledge enlightening discussions with P. Armbruster, H. Feldmeier and A. Kelic-Heil. G.M.P. is partly supported by the Deutsche Forschungsgemeinschaft through contract SFB 634 and the Helmholtz International Center for FAIR within the framework of the LOEWE program launched by the state of Hesse. I.V.P. is supported by the Russian government grant 11.G34.31.0047. P.-G.R. is supported by the BMBF under contract 06 ER 9063. F.-K.T. research is funded by the Swiss National Science Foundation (SNF) and a Humboldt Research Award. This joint collaboration benefitted from the EU FP7 infrastructure grant ENSAR/THEXO, the collaborative research program Eurogenesis (ESF), the Helmholtz Association through the Nuclear Astrophysics Virtual Institute (VH-VI-417), and the SNF program SCOPES for joint research with Eastern Europe.

References

- Myers, W.D., Swiatecki, W.J., Nucl. Phys. 81 (1966), 1
- Sobiczewski, A., Gareev, F.A., Kalinkin, B.N., Phys. Lett. 22 (1966), 500
- Meldner, H.W., Phys. Rev. C 178 (1969), 1815
- Nilsson, S.G., Thompson, S.G., Tsang, C.F., Phys. Lett. B 28 (1969), 458
- Nilsson, S.G., Tsang, C.F., Sobiczewski, A., Szymanski, Z., Wycech, S., Gustafson, C., Lamm, L.L., Moller, P., Nilsson, B., Nucl. Phys. A 131 (1969), 1
- Grummann, J., Fink, B., Mosel, U., Greiner, W., Z. Phys. 228 (1969), 371
- Brueckner, K.A., Chirico, J.H., Meldner, H.W., Phys. Rev. C 4 (1971), 732
- Cwiok, S., Dobaczewski, J., Heenen, P.-H., Magierski, P., Nazarewicz, W., Nucl. Phys. A 611 (1996), 211
- Bender, M., Rutz, K., Reinhard, P.-G., Maruhn, J.A., Greiner, W., Phys. Rev. C 60 (1999), 034304
- Kruppa, A.T. et al. Phys. Rev. C 61 (2000) 034313
- Heenen, P.-H., Nazarewicz, W., Europhys. News 33 (2002), 1
- Cwiok, S., Heenen, P.-H., Nazarewicz, Nature 433 (2005), 705
- M. Bender, W. Nazarewicz, and P.-G. Reinhard, Phys. Lett. B 515 (2001) 42
- Möller, P., Nix, J.R., J. Phys. G. 20 (1994), 1681
- Möller, P., Sierk, A.J., Ichikawa, T., Iwamoto, A., Bengtsson, R., Uhrenholt, H., Aringberg, S. Phys. Rev. C 79 (2009), 064304
- Möller, P. Int. J. Mod. Phys. E 19 (2010), 575
- Sobiczewski, A., Rozmej, P. Int. J. Mod. Phys. E 20 (2011), 325
- Erler, J. Langanke, K., Loens, H.P., Martínez-Pinedo, G. and Reinhard, P.G., Phys. Rev. C 85, 025802 (2012)
- Hofmann, S. Münzenberg, G., Rev. Mod. Phys. 72 (2000), 733
- Armbruster, P., Ann. Rev. Nucl. Part. Sci 50 (2000), 411
- Oganessian, Y.T., Nucl. Phys. 734 (2004), 109
- Moody, K. et al., Nucl. Phys. 734, (2004), 188
- Hofmann, S., Lect. Notes Phys. 764 (2009), 203
- Oganessian, Y.T. et al., Phys. Rev. C 74, 044602 (2006)
- Oganessian, Y.T. et al., Phys. Rev. Lett. 104 (2010), 142502
- Oganessian, Y.T. et al. Phys. Rev. C 83 (2011), 054315
- Schramm, D.N., Fowler, W.A., Nature 231 (1971), 103
- Flerov G.N., Ter-Akopian, G.M., Reports on Progress in Physics 46 817 (1983).
- Cowan, J.J., Thielemann, F.-K., Truran, J.W., Phys. Rep. (1991), 1
- Arnould, M., Goriely, S., Takahashi, K. Phys. Rep. 450 (2007), 97
- Thielemann, F.-K. et al., Prog. Part. Nucl. Phys. 66 (2011), 346
- Meldner, H.W. Phys. Rev. Lett. 28 (1972), 975
- Dorn, D.W., Hoff, R.W., Phys. Rev. Lett., 14 (1965), 440
- Bell, G.I., Rev. Mod. Phys. 39 (1967), 59
- Igley, J.S., Nucl. Phys. A, 124 (1969), 130
- Becker, S. A., in *Origin and Evolution of the Elements*, Carnegie Observatories Astrophysics Series, eds. A. McWilliam, M. Rauch (2004)
- Boleu, R., Nilsson, S.G., Sheline, R.K., Takahashi, K., Phys. Lett. 40B (1972), 517
- Schramm, D.N., Fizet, E.O., Ap.J. 180 (1973), 551
- Brueckner, K.A., Chirico, J.H., Jona, S., Meldner, H.W., Schramm, D.N., Seeger, P.A., Phys. Rev. C 7 (1973), 2133
- Howard, W.M., Nix, J.R., Nature 247 (1974), 17
- Howard, W.M., Moller, P., At. Data Nucl. Data Tables 25 (1980), 219
- Thielemann, F.-K., Metzinger, J., Klapdor, H.V., Z. Phys. A 309 (1983), 301
- Thielemann, F.-K., Metzinger, J., Klapdor, H.V., Astron. Astrophys. 123 (1983), 162
- Hilf, E.R., von Groote, H., Takahashi, K., Proc. 3rd Inter. Conf. on Nuclei far from Stability (Cargese), CERN 76-13 (1976), p. 142.
- Mamdouh A., Pearson, J.M., Rayet, C.M., Tondeur, F. Nucl. Phys. A 679 (2001) 337.
- Cowan, J.J., Pfeiffer, B., Kratz, K.-L., Thielemann, F.-K., Sneden, C., Burles, S., Tytler, D., Beers, T.C., Ap.J. 521 (1999), 194
- Mamdouh, A., Pearson, J.M., Rayet, M., Tondeur, F., Nucl. Phys. A 644 (1998), 389
- Myers, W.D., Swiatecki, W.J., Phys. Rev. C 60 (1999), 014606
- Goriely, S., Hilaire, S., Koning, A.J., Sin, M., Capote, R., Phys. Rev. C 79 (2009), 024612; Capote, R. et al., Nucl. Data Sheets 110 (2009), 3107 and <http://www-nds.iaea.org/RIPL-3/>
- Panov, I.V., Kolbe, E., Pfeiffer, B., Rauscher, T., Kratz, K.-L., Thielemann, F.-K., Nucl. Phys. A 747 (2005), 633
- Panov, I.V., Korneev, I.Y., Rauscher, T., Martínez-Pinedo, G., Kelic-Heil, A., Zinner, N.T., Thielemann, F.-K., Astron. Astrophys. 513 (2010), A61
- Panov, I.V., Korneev, I.Y., Thielemann, F.-K., Phys. Atom. Nucl. 72 (2009), 1026
- Petermann, I. et al., J. Phys. Conf. Ser. 202 (2010), 012008
- Langanke, K., Martínez-Pinedo, G., Petermann, I., Thielemann, F.-K., Prog. Part. Nucl. Phys. 66 (2011), 319
- Rauscher, T., Thielemann, F.-K., At. Data Nucl. Data Tables, 75 (2000), 1; 79 (2001), 47; 88 (2004), 1
- Mocelj, D., Rauscher, T., Martínez-Pinedo, G., Langanke, K., Pacearescu, L., Faessler, A., Thielemann, F.-K., Alhasid, Y., Phys. Rev. C 75 (2007), 045805
- Loens, H. P., Langanke, K., Martínez-Pinedo, G., Rauscher, T., Thielemann, F.-K., Phys. Lett. B, 666 (2008), 395

58. Litvinova, E., Loens, H. P., Langanke, K., Martínez-Pinedo, G., Rauscher, T., Ring, P., Thielemann, F.-K., Tselyaev, V., Nucl. Phys. A, 823 (2009), 26
59. Cyburt, R. H., et al., Astrophys. J. Suppl., 189 (2010), 240
60. Rauscher, T., Int. J. Mod. Phys. E (2011), 20 (2011), 1071
61. Goriely, S., Hilaire, S., Koning, A. J., Astron. Astrophys., 487 (2008), 767
62. Larsen, A. C., Goriely, S., Phys. Rev. C82 (2010), 014318
63. Goriely, S., Hilaire, S., Koning, A. J., Capote, R., Phys. Rev. C83 (2011), 034601
64. Kodama, T., Takahashi, K., Nucl. Phys. A 239 (1975), 489
65. Ren, Z., Xu, C., Nucl. Phys. A 759 (2005), 64
66. Smolańczuk, R., Skalski, J., Sobiczewski, A., Phys. Rev. C52 (1995), 1871
67. Smolańczuk, R., Phys. Rev. C, 56 (1997), 812
68. Möller, P., Nix, J.R., Myers, W.D., Swiatecki, W.J., At. Data Nucl. Data Tables 59 (1995), 185
69. Aboussir, Y., Pearson, J.M., Dutta, A.K., Tondeur, F., At. Data Nucl. Data Tables, 61 (1995), 127
70. Duflo, J., Zuker, A. P., Phys. Rev. C, 52 (1995), 23
71. Goriely, S., Chamel, N., Pearson, J.M., Phys. Rev. Lett., 102 (2009), 152503
72. Goriely, S., Chamel, N., Pearson, J. M., Phys. Rev. C, 82 (2010), 035804
73. Sheikh, J.A. Nazarewicz, W., Pei, J.C., Phys. Rev. C **80**, 011302 (2009)
74. Goriely, S., Samyn, M., Pearson, J.M., Phys. Rev. C **75** (2007) 064312.
75. Martínez-Pinedo, G., et al., Prog. Part. Nucl. Phys. 59 (2007), 199
76. Sobiczewski, A., Patyk, Z., Cwiok, S., Phys. Lett. B **224** (1989) 1
77. Möller, P., Pfeiffer, B.,Kratz, K.-L., Phys. Rev. C **67** (2003) 055802
78. Zinner, N.T., PhD Thesis, University of Aarhus, Denmark (2007)
79. Gaimard, J.-J., Schmidt, K.-H., Nucl. Phys. A 531 (1991), 709
80. Benlliure, J. Grewe, A., de Jong, M., Schmidt, K.-H., Zhdanov, S., Nucl. Phys. A 628 (1998), 458
81. Lattimer, J. M., & Schramm, D. N., Astrophys. J.210 (1976), 549
82. Lattimer, J. M., Mackie, F., Ravenhall, D. G., & Schramm, D. N., Astrophys. J.213 (1977), 225
83. Freiburghaus, C., Rosswog, S., Thielemann, F.-K., Astrophys. J.525 (1999), L121
84. Goriely, S., Bauswein, A., & Janka, H.-T., arXiv:1107.0899 (2011)
85. Cameron, A.G.W., Astrophys. J. **587** (2003) 327.
86. Fujimoto, S., Nishimura, N. & Hashimoto, M., Astrophys. J.680 (2008), 1350
87. Winteler, C. *et al.*, Astrophys. J. **750** L22 (2012).
88. Woosley, S. E. Wilson, J. R., Mathews, G. J., Hoffman, R. D., Meyer, B. S. Astrophys. J.433 (1994), 229
89. Takahashi, K., Witt, J. & Janka, H.-T. Astron. Astrophys.286 (1994), 857
90. Qian, Y.-Z. & Woosley, S. E. Astrophys. J., 471 (1996), 331
91. Otsuki, K., Tagoshi, H., Kajino, T., Wanajo, S., Astrophys. J. **533**, 424 (2000).
92. Thompson, T.A., Burrows, A., Meyer, B.S., Astrophys. J. **562**, 887 (2001).
93. Arcones, A., Janka, H.-T., Scheck, L., Astron. & Astrophys. **467**, 1227 (2007).
94. Farouqi, K., Kratz, K.-L., Pfeiffer, B., Rauscher, T., Thielemann, F.-K., Truran J.W., , Astrophys. J. **712**, 1359 (2010).
95. Arcones, A., Martínez-Pinedo, G., Phys. Rev. C **83**, 045809 (2011).
96. Fischer, T., Whitehouse, S.C., Mezzacappa, A., Thielemann, F.-K., Liebendörfer, M., Astron. Astrophys. **517**, A80 (2010).
97. Hüdepohl, L., Müller, B., Janka, H.-T., Marek, A., Raffelt, G., Physical Review Letters 104, 251101 (2010).
98. Surman, R., McLaughlin, G. C., Ruffert, M., Janka, H.-T., & Hix, W. R., Astrophys. J., 679 (2008), L117
99. Wanajo, S., & Janka, H.-T., arXiv:1106.6142 (2011)
100. Arcones, A., Janka, H.-Th. & Scheck, L. Astron. Astrophys., 467 (2007), 1227
101. Meyer, B.S., Brown, J.S., Astrophys. J. Suppl. **112** (1997) 199.
102. Panov, I.V., Janka, H.-T., Astron. & Astrophys. **494** (2009) 829.
103. Wanajo, S., Janka, H.-T., Kubono, S., Astrophys. J. **729**, 46 (2011)
104. Timmes, F.X., Arnett, D., Astrophys. J. Suppl. **125** (1999) 277.
105. Hix, W.R., Thielemann, F.-K., J. Comp. Appl. Math. 109 (1999), 321
106. Sasaqui, T., Otsuki, K., Kajino, T., Mathews, G.J., Astrophys. J. **645** (2006) 1345.
107. Burbidge, E.M., Burbidge, G.R., Fowler, W.A., Hoyle, F., Rev. Mod. Phys. **29** (1957) 547.
108. Cameron, A.G.W., Stellar evolution, nuclear astrophysics, and nucleogenesis, Report CRL-41, Chalk River (1957).
109. Blake, J.B., Schramm, D.N., Astrophys. J. **209** (1976) 846.
110. Wanajo, S., Astrophys. J. **666** (2007) L77.